Influences of periodic mechanical deformation on pinned spiral waves

Jiang-Xing Chen, Liang Peng, Qiang Zheng, Ye-Hua Zhao, and He-Ping Ying

Citation: Chaos **24**, 033103 (2014); doi: 10.1063/1.4886356
View online: http://dx.doi.org/10.1063/1.4886356
View Table of Contents: http://scitation.aip.org/content/aip/journal/chaos/24/3?ver=pdfcov
Published by the AIP Publishing

Influences of periodic mechanical deformation on pinned spiral waves

Jiang-Xing Chen,[1,a)] Liang Peng,[1] Qiang Zheng,[1] Ye-Hua Zhao,[2,a)] and He-Ping Ying[3,a)]
[1]*Department of Physics, Hangzhou Dianzi University, Hangzhou 310018, China*
[2]*Department of Mathematics, Hangzhou Dianzi University, Hangzhou 310018, China*
[3]*Department of Physics, Zhejiang University, Hangzhou 310027, China*

(Received 8 December 2013; accepted 20 June 2014; published online 2 July 2014)

In a generic model of excitable media, we study the behavior of spiral waves interacting with obstacles and their dynamics under the influences of simple periodic mechanical deformation (PMD). Depending on the characteristics of the obstacles, i.e., size and excitability, the rotation of a pinned spiral wave shows different scenarios, e.g., embedding into or anchoring on an obstacle. Three different drift phenomena induced by PMD are observed: scattering on small partial-excitable obstacles, meander-induced unpinning on big partial-excitable obstacles, and drifting around small unexcitable obstacles. Their underlying mechanisms are discussed. The dependence of the threshold amplitude of PMD on the characteristics of the obstacles to successfully remove pinned spiral waves on big partial-excitable obstacles is studied. © *2014 AIP Publishing LLC*. [http://dx.doi.org/10.1063/1.4886356]

Exploring the properties of pinned spiral waves has attracted much attention in the past decade. The characteristics of a defect, such as excitability and size, may determine the dynamics of a pinned spiral wave. Insight into their interaction will contribute to develop strategies to eliminate pinned spirals that are responsible for cardiac tachycardia. On the other hand, the behavior of a pinned spiral wave is also greatly affected by the mechanical deformation of the medium, such as periodic stretching and contracting of a heart muscle. However, the effects are still not completely understood and remain an area of active investigation. Studies on this field will benefit the understanding of the dynamics of pinned spirals in cardiac tissue.

I. INTRODUCTION

Rotating spiral waves have been observed in many biological, physical, and chemical systems,[1,2] such as cardiac tissue,[3,4] the Belousov-Zhabotinsky (BZ) reaction,[5,6] Dictyostelium discoideum amoebae,[7] the animal retinas,[8] and catalytic oxidation of CO.[9] Heterogeneities in those systems play an important role in the formation of spiral waves.[10–12] For example, fibrosis and ischemia in heart tissue generally lead to the emergency of pinned spiral waves that are responsible for cardiac tachycardia.[13]

Once a spiral wave is pinned on heterogeneity, it is not easy to be removed.[14] Understanding the dynamics of pinned spirals and developing strategies to eliminate them have attracted much attention. Two methods suppressing pinned spiral waves should be mentioned in this field for their efficacy and practicability. One is the successful application of a train of high-frequency stimuli to suppress pinned spiral waves, which is called antitachycardia pacing (ATP) in the wide clinical use. However, its mechanism is still not completely understood and remains an area of active investigation.[15–20] Another recent concerned topic to unpin spiral is based on the electric field-induced wave emission from heterogeneities (WEH).[21–25] The success of unpinning is frequency-dependent and sensitive to the initial position of the spiral.

On the other hand, mechanoelectrical feedback is regarded as one of the important factors that affect the electrical excitation in cardiac tissue.[26–29] Panfilov *et al.*[29,30] investigated deformation-induced breakup of spiral waves as well as drift by applying a Reaction-Diffusion-Mechanics model. Munũzuri *et al.*[31] designed elastic excitable medium by incorporating the BZ reaction into a polyacrylamide-silica gel to investigate the effect of mechanical deformation on spiral waves. They reported resonant drift of a spiral wave when its rotation frequency is equal to that of the deformation. Recently, Cherubini *et al.*[32] found that the deformation plays a nonprominent role in the process of unpinning by ATP. However, the influences of periodic mechanical deformation (PMD) on spiral waves interacting with heterogeneities are still open. Interesting questions include whether the pinned spiral can be removed through drifting by PMD and what the conditions are.

In this paper, we will investigate numerically the influences of PMD on a spiral wave interacting with heterogeneity in a simple excitable model. The conditions how to induce the pinned spiral to drift are focused on. On the one hand, the effects of amplitude and frequency of PMD are explored. On the other hand, the roles of characteristics of obstacles, such as radius and excitability, are studied in the unpinning process.

II. MODEL

The simulation of an excitable medium is performed in terms of a modified FitzHugh-Nagumo model (the Barkley model[33])

[a)]Authors to whom correspondence should be addressed. Electronic addresses: jxchen@hdu.edu.cn; yhzhao@hdu.edu.cn; and hpying@zju.edu.cn.

$$\frac{\partial u}{\partial t} = f(u,v) + \nabla^2 u,$$
$$\frac{\partial v}{\partial t} = g(u,v), \tag{1}$$

where u denotes fast activator and v represents slow inhibitory variable. The functions $f(u,v) = \frac{u(1-u)}{\varepsilon}(u - \frac{(v+b)}{a})$ and $g(u,v) = (u - v)$ describe the local kinetics. Parameter ε determines the ratio of characteristic time scales of the activator and inhibitor variables. Numerical simulations are carried out on 256×256 grid points employing the explicit Euler method. The space and time steps are $\Delta x = \Delta y = 0.390625$ (i.e., an area 100×100) and $\Delta t = 0.02$, respectively. No-flux conditions are imposed on the boundaries.

This model catches the essential features of excitable media. The parameters a and b determine the excitation threshold (b/a). We set $\varepsilon = 0.02$ and $a = 0.7$ while changing the value of b in order to tune the excitability of the medium. With suitable initial condition, a spiral wave can be developed. The free (unpinned) spiral tip shows a circular trajectory with radius R_0 and rotating frequency ω_0. In Fig. 1, we present the dependence of frequency ($\omega_0(b)$) and core radius ($R_0(b)$) of a spiral wave on the value of b. One can find that the increase of b leads to reduction of ω_0 and rapid increase of R_0.

The shape of the heterogeneity (obstacle) in the simulation is chosen to be a circle with a radius R_H. Outside of the circle ($r > R_H$), we fix $b_{out} = 0.1$. Inside of the obstacle ($r \le R_H$), we set $b_{in} > b_{out}$ so that the excitability threshold b/a inside is larger than that outside (the obstacle is less excitable). An unexcitable obstacle is with $b_{in} = a/2 = 0.35$ and a partially unexcitable obstacle is with $b_{out} < b_{in} < a/2$. We put the obstacle on the center of the spiral tip core.

The mechanical deformation of a medium can be modeled by an operation where any fixed point $\mathbf{r}$ of the medium is changed to $\mathbf{r}'$. Here, we consider a simple oscillation $\mathbf{r}' = x(1 + A\cos(\omega_d t + \phi))\mathbf{i} + y(1 + A\cos(\omega_d t + \phi))\mathbf{j}$ with A the amplitude, ω_d the frequency, and ϕ the initial phase, respectively.[31,34] Then, Eq. (1) is modified to be

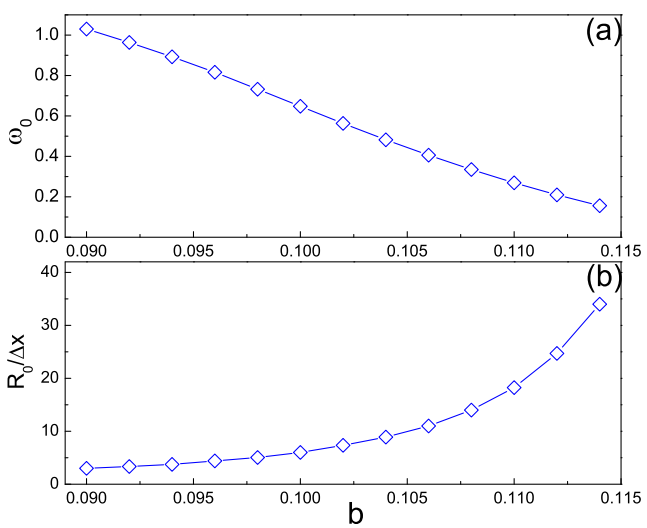

FIG. 1. Dependence of frequency (ω_0) and core radius (R_0) of a spiral wave on parameter b. (a) ω_0 vs. b. (b) $R_0/\Delta x$ vs. b.

$$u_t = f(u,v) + \frac{u_{xx}}{[1 + A\cos(\omega_d t + \phi)]^2} + \frac{u_{yy}}{[1 + A\cos(\omega_d t + \phi)]^2},$$
$$v_t = g(u,v). \tag{2}$$

III. RESULTS AND DISCUSSIONS

A. Dynamics of pinned spiral waves characterized by obstacles

Before performing deformation on the medium, we study the behavior of a spiral wave pinned on an obstacle. We label R_{in} (R_{out}) the core radius of spiral tip in a homogeneous medium with parameters equal to those inside (outside) the obstacle. Then, $R_{in} > R_{out}$ is an equivalent condition of $b_{in} > b_{out}$. Note that there are two relations: $R_{out} = R_0(0.1)$ and $\omega_{out} = \omega_0(0.1)$, since the condition $b_{out} = 0.1$ is fixed in our simulation. The obstacle is characterized by two factors: size (radius R_H) and excitability (b_{in}).

When the R_H is smaller than R_{out}, the real core of a pinned spiral (R_{PS}) is equal to R_{out}. The spiral tip does not touch the obstacle. As R_H is increased across R_{out} ($R_H/R_{out} > 1.0$), R_{PS} is gradually expanded. Two examples are shown in Fig. 2(a) where an unexcitable obstacle ($b_{in} = 0.35$) and a partial-excitable case ($b_{in} = 0.11$) are presented. There are differences between these two cases. In the unexcitable case, the tip will rotate around the boundary of an obstacle with radius $R_{ps} \approx R_H$. From the case in Fig. 2(a), one can find this point: the fit curve with slope 1.0 (namely, $R_H = R_{ps}$) coincides with the simulated data. From Fig. 2(d), it is shown that the trajectory of the tip with radius R_{ps} is exactly on the boundary of the obstacle with radius R_H. The underlying mechanism has been discussed by Pazó *et al.*[14] However, in the partial-excitable case, the outward force from the condition $R_{in} > R_H$ (instead of $R_{in} \gg R_H$ in Ref. 14) is not strong enough to force the tip out of the obstacle completely. That is because there is also the inward force from the condition $R_H > R_{out}$, which results in $R_H > R_{ps}$. Likewise, the tip in the obstacle cannot move freely as that in homogeneous medium with $b = b_{out}$ due to the outward force from the condition $R_{in} > R_H$, which results in $R_{out} < R_{ps}$. Then, the real situation should be $R_{out} < R_{ps} < R_H$. A corresponding example is shown in Fig. 2(c) where one can find that the spiral embeds into the obstacle. Correspondingly, in the case with $b_{in} = 0.11$ in Fig. 2(a), the slope in $R_{ps}/R_{out} - R_H/R_{out}$ curve is much smaller than 1.0. Note that the value of R_{ps}/R_{out} saturates at large R_H/R_{out} since R_{ps} approaches R_{in} when R_H is continuously increased.

Due to the expansion of the spiral core, its frequency is decreased correspondingly. In Fig. 2(b), we plot the frequency of pinned spiral (ω_{ps}) when the size of obstacle is increased. Compared with the partial-excitable case ($b_{in} = 0.11$), the decrease of frequency in unexcitable case ($b_{in} = 0.35$) is faster.

B. Influences of PMD on spiral waves in homogeneous excitable medium

The frequency of PMD (ω_d) plays a key role in modulating the motion of the spiral wave, which is presented in

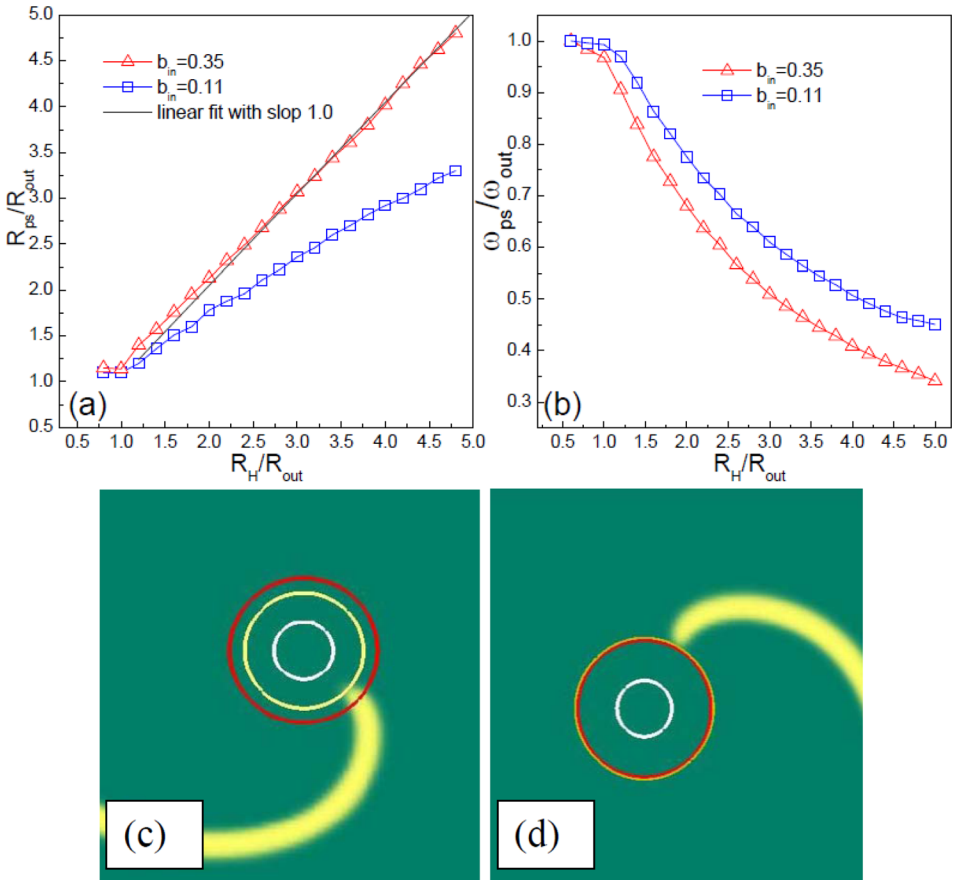

FIG. 2. Dependence of radius (R_{ps}) and frequency (ω_{ps}) of a pinned spiral wave on the size of an obstacle, which is shown in (a) R_{ps}/R_{out} vs. R_H/R_{out} curves and (b) ω_{ps}/ω_{out} vs. R_H/R_{out} curves. A pinned spiral rotates with radius R_{ps} on an obstacle ($R_H/R_{out}=2.5$) with (c) $b_{in}=0.11$ and (d) $b_{in}=0.35$. Three circles from the inside to outside with radius R_{out}, R_{ps}, and R_H are shown in (c) and (d), respectively. In (d), the circle R_{ps} coincides with R_H.

Fig. 3 where the $r_2/r_1 - \omega_d/\omega_0$ plane with weak amplitude ($A=0.05$) is displayed. r_1 is the radius of a primary orbit and r_2 denotes the radius of a modulation orbit (see the schematic measurement in Fig. 3). When the frequency of PMD is equal to that of the spiral wave, resonant drift occurs (see the trajectory at $\omega_d/\omega_0=1.0$). If ω_d deviates from ω_0, the orbits show inward petals ($\omega_d<\omega_0$, see trajectory of $\omega_d/\omega_0=0.969$) and outward petals ($\omega_d>\omega_0$, see trajectory of $\omega_d/\omega_0=1.03$). The modulation radius r_2 decreases rapidly in this deviation. From the trajectories at $\omega_d/\omega_0=0.465$ and 1.86, one can find that the radius approaches primary value r_1 (now, $r_2\to 0$). After fitting the data in Fig. 3, we get a perfect quantitative expression $r_2/r_1 \propto (1-\omega_d/\omega_0)^{-1}$, which is consistent with the results reported by Mikhailov *et al.*[35] when a spiral wave is influenced by weak periodic perturbation.

C. Scattering of spiral waves by PMD on small partial-excitable obstacles

Now, we can focus on the influences of PMD on spirals interacting with obstacles and the conditions how to remove them. From the discussion mentioned above, it is known that the characteristics of an obstacle (R_H and b_{in}) may determine the frequency of the pinned spiral. To study the deformation-induced drift of a pinned spiral, one condition should be fulfilled: $\omega_d=\omega_{out}$. So that, once the pinned spiral leaves the obstacle, it can show resonant drift and move away. This condition is fixed when we study their interactions.

At first, we study the case when the obstacle is partial-excitable and the size is small ($R_H<R_{out}$). In Fig. 4, an example is presented. The PMD induces the spiral to drift. It is shown that the direction of drift changes (see the two arrows in Fig. 4) once the tip enters into the obstacle region in which the tip has bigger curvature radius. Thus, when a spiral wave meets small partial-excitable obstacles, it may be scattered on them by changing the direction of drift.

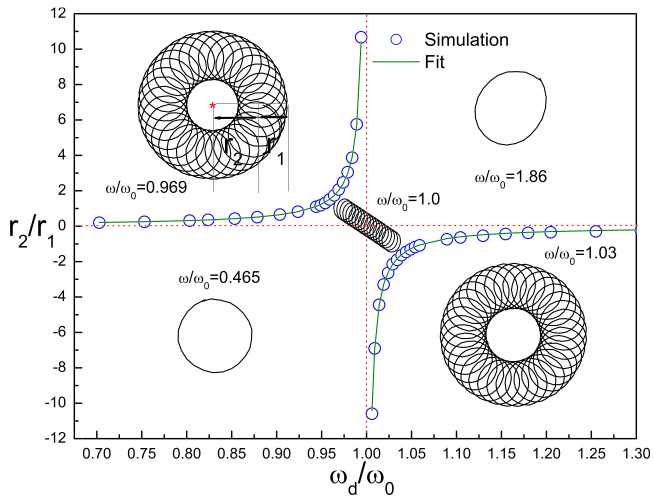

FIG. 3. Dependence of meandering tip radius on the frequency of PMD. Ratio r_2/r_1 is controlled by parameter ω_d/ω_0, where r_1 is the radius of a primary orbit and r_2 a modulation orbit, respectively. The measurement of r_1 and r_2 is indicated in the figure. Note that r_2 is set to be positive (negative) in inward (outward) meandering. The circles are plotted from simulation and the solid lines are fitting curves according to $r_2/r_1 \propto 1/(1-\omega_d/\omega_0)$. The amplitude of PMD is 0.05. Corresponding orbits are shown in the insets. The value of b is 0.1.

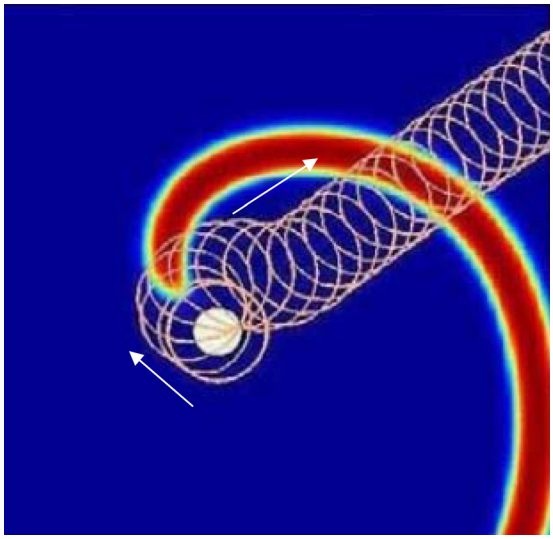

FIG. 4. The interaction of a spiral wave and a partial-excitable small obstacle. The obstacle (characterized by $R_H/R_{out}=0.5$ and $b_{in}=0.115$) is denoted by the white circle. The two auxiliary arrows show the changed direction of drift. The spiral wave is plotted at time when the deformation with $\omega_d=\omega_0$ and $A=0.11$ is applied.

D. Interactions between a pinned spiral and a big partial-excitable obstacle and unpinning dynamics based on meander-induced mechanism

When the size of the obstacle is increased, the spiral wave embeds into the obstacle, i.e., $R_{out}<R_{ps}<R_H$. In Fig. 5(a), we show the trajectory of spiral tip from $t=80$ to $t=100$ before the deformation is applied at $t=100$. Due to the condition $\omega_d>\omega_{ps}$ (the condition $\omega_d=\omega_{out}$ is fixed), the spiral tip begins to meander showing outward rotating petals, which has been illustrated in Fig. 5(b). This phenomenon is consistent with the illustration in Fig. 3. With the evolution of time, the meandering behavior becomes more and more pronounced, which can be seen in Fig. 5(c). This also can be found in Fig. 5(d) where the distance from the spiral tip to the core of the obstacle fluctuates with increasing amplitude after $t=100$. Once the trajectory of tip has the chance to entirely move out of the obstacle, it is driven away for resonant drift. One can find this point in the process in Fig. 5(c).

The threshold amplitude of PMD for removing the pinned spiral increases as the size of the obstacle. The results from simulation are presented in Fig. 6(a). Since the removing of pinned spiral is based on the meandering mechanism, it is evident to understand this point: increasing A_C will make the meandering more pronounced, which has been illustrated in Fig. 6(b). In each b_{in} in Fig. 6(a), one can find that there is a maximal radius $R_{H,max}$ beyond which the PMD cannot successfully remove the pinned spiral any more. The reason is that increasing amplitude further will make the spiral breakup.[34] The value of $R_{H,max}$ decreases when b_{in} is increased (see Fig. 6(c)).

In a same obstacle whether R_H/R_{out} is bigger than 1.0 or not, a bigger value of b_{in} leads to a bigger A_c, which has been presented in Fig. 6(d). It can be also interpreted clearly by the meandering mechanism: on the one hand, the meandering behavior is difficult when b_{in} is bigger (think about the limit case $b_{in}=0.35$ where the spiral tip is restricted on the boundary and cannot meander into the obstacle); on the other hand, bigger b_{in} results in smaller ω_{ps}/ω_{out} (see Fig.

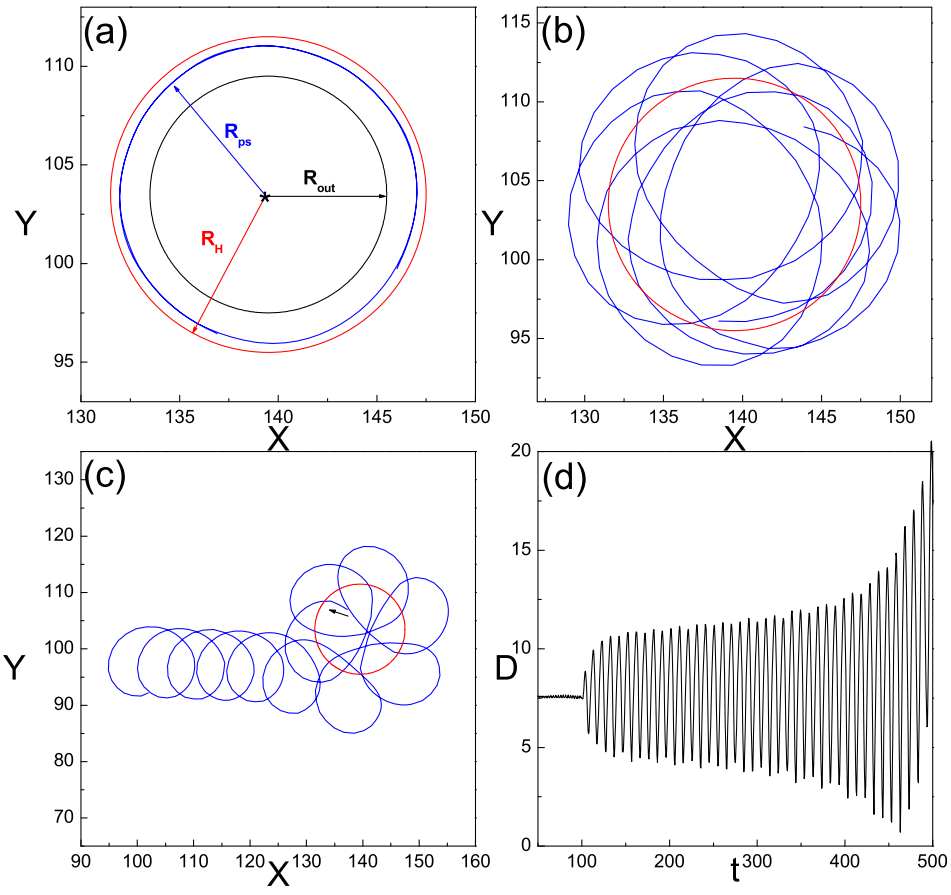

FIG. 5. (a)–(c) The evolution of trajectory of a spiral tip under the influence of PMD with $\omega_d=\omega_{out}$ and $A=0.21$ in different periods of time. The obstacle with $R_H/R_{out}=4/3$ and $b_{in}=0.11$ is denoted by the dotted circle. Data are plotted from (a) $t=80$ to $t=100$, (b) $t=100$ to $t=175$, and (c) $t=432$ to $t=550$. (d) The evolution of distance from the spiral tip to the core of the obstacle. The PMD is applied at $t=100$.

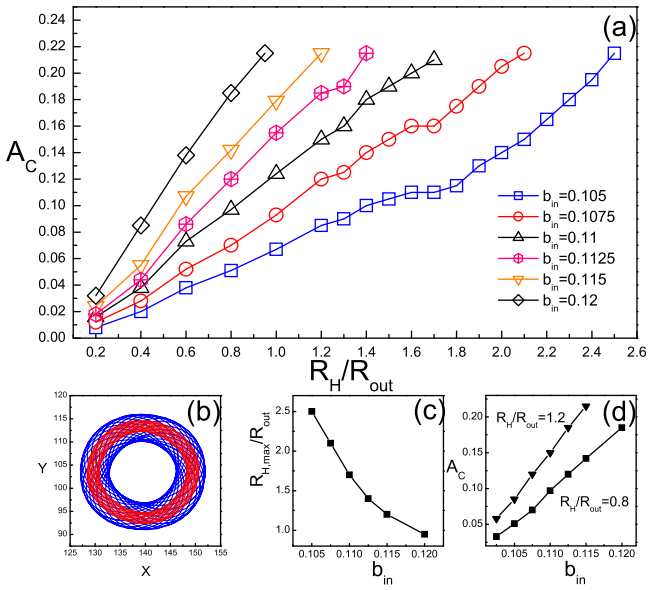

FIG. 6. (a) The dependence of threshold amplitude A_c on radius (R_H/R_{out}) and excitability (b_{in}). (b) Trajectories of meandering spiral tips with different amplitudes. The smaller circle (red) is trajectory resulted from $A = 0.11$, while the bigger circle (blue) from $A = 0.21$. (c) Plotted $R_{H,max}/R_{out}$ vs. b_{in} curve. (d) $A_c - b_{in}$ curves with $R_H/R_{out} = 1.2$ and $R_H/R_{out} = 0.8$.

2(b)), make its value deviates from 1.0 (resonant frequency) more. Consequently, it reduces the meandering behavior (see Fig. 3). Thus, bigger A_C is required when b_{in} is increased. The interpretation also accounts for the increase of slope in $R_H/R_{out} - A_C$ curves as b_{in} is increased in Fig. 6(a) and $A_C - b_{in}$ as R_H is increased in Fig. 6(d) (comparing the curve $R_H/R_{out} = 1.2$ with $R_H/R_{out} = 0.8$).

E. Removing spiral waves from small unexcitable obstacles based on drift-around mechanism

A pined spiral wave cannot enter into an unexcitable obstacle. Thus, the mechanism of meander-induced unpinning in the case $R_H > R_{out}$ fails. Even in the case $R_H < R_{out}$, the spiral will be pinned on the unexcitable obstacle. This phenomenon is different from the scatting behavior on small partial-excitable obstacles. An example is shown in Fig. 7(a). A tip starts to display resonant drift by PMD from the point "0." Since the drift is not fast enough (or the obstacle is too big), the tip collides with the obstacle at point "1" after one period (see the first loop). Subsequently, the spiral moves along the star line (see the second loop). The tip collides with the obstacle again at point "2." Eventually, the spiral wave is pinned with meandering trajectory (see the inset). However, if the spiral can drift fast by PMD (or the obstacle is small), the tip can be unpinned by moving around the obstacle. In Fig. 7(b), an example is plotted to display this process. At the point "0," the spiral wave starts to drift by PMD. The tip moves from point "1" to "3" after one rotating period (see the tip trajectory after PMD). Since the obstacle is small this time, the tip drifts around it and then moves away. No collision between the tip and obstacle occurs, which is different from the case in Fig. 7(a).

The distance between points "1" and "3" ($R_{1,3}$) illustrates the displacement of the tip in one period. For a fixed A, the value $R_{1,3}$ means the maximal diameter of an obstacle

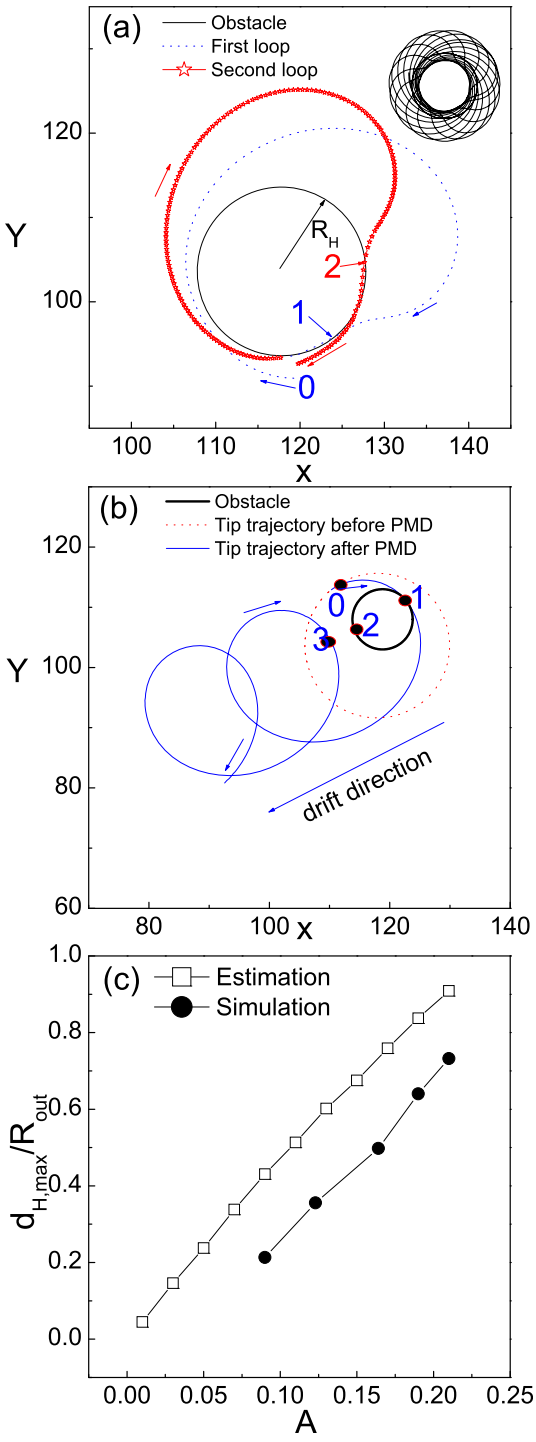

FIG. 7. (a) Motion of a spiral tip pinned on an obstacle (the black solid circle) with $R_H/R_{out} = 0.76$ and $b_{in} = 0.35$. The number "0" denotes the start point at which the tip begins to drift induced by PMD. The blue dotted trajectory, colliding with the obstacle at point "1," is the first loop of the tip motion. The red star line shows the second loop which collides with the obstacle at point "2." Other arrows show the directions of tip motion. The inset shows the corresponding long-time evolution of the tip trajectory. (b) The tip trajectory illustrates the process when it drift-around an obstacle with $R_H/R_{out} = 0.38$. Other parameters of the PMD in (a) and (b) are: $\omega_d = \omega_{out}$ and $A = 0.21$. (c) The dependence of $d_{H,max}$ on the amplitude A of PMD. The curve marked by circles is plotted from the simulation, while the curve marked by squares is plotted from the relation $d_{H,max} = 2\pi V/\omega_{out}$, where V is the drift velocity by PMD without obstacle. Note that the spiral wave will break as $A > 0.21$. Here, the simulation is carried on a system containing 240×240 grids with $\Delta x = 1/6$ and $\Delta t = 0.0025$.

($d_{H,max}$) above which the spiral cannot be unpinned. In Fig. 7(c), the values of $d_{H,max}$ under different A are plotted from the simulation (see the curve marked by circles). Evidently, the value can also be estimated from the relation $d_{H,max} = 2\pi V/\omega_{out}$, where V is the corresponding drift velocity. After simulating the values of V under different A, one can obtain a $d_{H,max}$-A curve in Fig. 7(c) (see the curve marked by squares). It is shown that the values from the simulation are smaller than that from the estimation. That is because a fragment is cut off from the drifting spiral temporarily when the tip moves to "3" (roughly denoted by the distance from the point "2" to "3," see Fig. 7(b)). The fragment may shrink if its length is shorter than a certain critical value.[20] Compared with the cases of the partial-excitable obstacles in Fig. 6, the maximal sizes in Fig. 7(c) are very small. We assume that it is one plausible reason why it is difficult to unpin spirals from unexcitable obstacles in cardiac tissue which keeps on stretching and contracting.

IV. CONCLUSION

In conclusion, we have studied the behavior of spiral waves interacting with obstacles and their dynamics under the influences of PMD. Dependence of meandering tip radius on the frequency of PMD is presented in the $r_2/r_1 - \omega_d/\omega_0$ plane. Resonant drift by PMD is studied to remove the pinned spirals. When the obstacle is partial-excitable, the direction of drift induced by PMD will be changed when a spiral wave passes through small obstacles ($R_H/R_{out} < 1$). When the obstacle is big ($R_H/R_{out} > 1$), the spiral may embed into the obstacle ($R_{out} < R_{ps} < R_H$). The increased meandering behavior induced by PMD results in the unpinning of spiral waves. That is to say, the underlying mechanism is meander-induced drift. The dependence of the threshold amplitude of PMD to induce the pinned spiral to drift on the characteristics of obstacles is illustrated in the $A_c - R_H/R_{out}$, $A_c - b_{in}$, and $A_c - R_{H,max}$ curves. For the unexcitable obstacles, the spiral wave may be anchored on the boundary of the obstacle. To avoid possible breakup, the amplitude of the PMD is small, which results in slow drift velocity. Thus, the spiral can only depart from certain small obstacles by drifting around them. We believe our results can be observed in chemical experiments such as the BZ reaction in gels. Because the heart is stretching and contracting all the time, we also hope the studies may give some contribution to understand the interaction between pinned spirals and obstacles in cardiac tissue.

ACKNOWLEDGMENTS

This work was supported by the National Natural Science Foundation of China (Grant Nos. 11005026 and 11274271), the Program for Qianjiang Talents in Zhejiang Province (Grant No. 2012R10057), and the Start-Up Fund for Returned Oversea Chinese Scholars (Grant No. 20121707).

[1]*Chemical Wave and Pattern*, edited by R. Kapral and K. Showalter (Kluwer Academic, Dordrecht, 1993).
[2]M. C. Cross and P. C. Hohenberg, Rev. Mod. Phys. **65**, 851 (1993).
[3]V. I. Krinsky, Biofizika **11**, 676 (1966).
[4]J. M. Davidenko, A. V. Pertsov, R. Salomonsz, W. Baxter, and J. Jalife, Nature (London) **355**, 349 (1992).
[5]A. T. Winfree, Science **175**, 634 (1972).
[6]V. K. Vanag and I. R. Epstein, Science **294**, 835 (2001).
[7]K. J. Lee, E. C. Cox, and R. E. Goldstein, Phys. Rev. Lett. **76**, 1174 (1996).
[8]A. Gorelova and J. Bures, J. Neurobiol. **14**, 353 (1983).
[9]S. Jakubith, H. H. Rotermund, W. Engel, A. von Oertzen, and G. Ertl, Phys. Rev. Lett. **65**, 3013 (1990).
[10]M. Bär, E. Meron, and C. Utzny, Chaos **12**, 204 (2002).
[11]G. Bub and A. Shrier, Chaos **12**, 747 (2002).
[12]I. Schebesch and H. Engel, Phys. Rev. E **57**, 3905 (1998).
[13]J. N. Weiss, Z. Qu, P. S. Chen, S. F. Lin, H. S. Karagueuzian, H. Hayashi, A. Garfinkel, and A. Karma, Circulation **112**, 1232 (2005).
[14]D. Pazó, L. Kramer, A. Pumir, S. Kanani, I. Efimov, and V. Krinsky, Phys. Rev. Lett. **93**, 168303 (2004).
[15]N. Bursac and L. Tung, Cardiovasc. Res. **69**, 381 (2006).
[16]C. M. Ripplinger, V. I. Krinsky, V. P. Nikolski, and I. R. Efimov, Am. J. Physiol.: Heart Circ. Physiol. **291**, H184 (2006).
[17]A. Isomura, M. Hörning, K. Agladze, and K. Yoshikawa, Phys. Rev. E **78**, 066216 (2008).
[18]T. Masanobu, I. Akihiro, M. Hörning, H. Kitahata, K. Agladze, and K. Yoshikawac, Chaos **19**, 043114 (2009).
[19]K. Agladze, M. W. Kay, V. Krinsky, and N. Sarvazyan, Am. J. Physiol.: Heart Circ. Physiol. **293**, H503 (2007).
[20]A. Pumir, S. Sinha, S. Sridhar, M. Argentina, M. Hörning, S. Filippi, C. Cherubini, and S. Luther, Phys. Rev. E **81**, R010901 (2010).
[21]J. Cysyk and L. Tung, Biophys. J. **94**, 1533 (2008).
[22]S. Takagi, A. Pumir, D. Pazó, I. Efimov, V. Nikolski, and V. Krinsky, Phys. Rev. Lett. **93**, 058101 (2004).
[23]S. Luther, F. H. Fenton, B. G. Kornreich *et al.*, Nature **475**, 235 (2011).
[24]P. Bittihn, G. Luther, E. Bodenschatz, V. Krinsky, U. Parlitz, and S. Luther, New J. Phys. **10**, 103012 (2008).
[25]P. Bittihn, A. Squires, G. Luther, E. Bodenschatz, V. Krinsky, U. Parlitz, and S. Luther, Philos. Trans. R. Soc., A **368**, 2221 (2010).
[26]A. V. Panfilov, R. H. Keldermann, and M. P. Nash, Phys. Rev. Lett. **95**, 258104 (2005).
[27]L. D. Weise and A. V. Panfilov, Phys. Rev. Lett. **108**, 228104 (2012).
[28]N. A. Trayanova, J. Constantino, and V. Gurev, J. Electrocardiol. **43**, 479 (2010).
[29]R. H. Keldermann, M. P. Nash, H. Gelderblom, V. Y. Wang, and A. V. Panfilov, Am. J. Physiol.: Heart Circ. Physiol. **299**, H134 (2010).
[30]A. V. Panfilov, R. H. Keldermann, and M. P. Nash, Proc. Natl. Acad. Sci. U. S. A. **104**, 7922 (2007).
[31]A. P. Munüzuri, C. Innocenti, J.-M. Flesselles, J.-M. Gilli, K. I. Agladze, and V. I. Krinsky, Phys. Rev. E **50**, R667 (1994).
[32]C. Cherubini, S. Filippi, and A. Gizzi, Phys. Rev. E **85**, 031915 (2012).
[33]D. Barkley, M. Kness, and L. S. Tuckerman, Phys. Rev. A **42**, R2489 (1990).
[34]J. X. Chen, J. R. Xu, X. P. Yuan, and H. P. Ying, J. Phys. Chem. B **113**, 849 (2009).
[35]A. S. Mikhailov, V. A. Davydov, and V. S. Zykov, Physica D **70**, 1 (1994).